J. Biochem. 2010;148(6):659–667 doi:10.1093/jb/mvq105

JB THE JOURNAL OF BIOCHEMISTRY

Functional proteomic analysis of promyelocytic leukaemia nuclear bodies in irradiation-induced MCF-7 cells

Received August 12, 2010; accepted August 24, 2010; published online September 7, 2010

Jinfeng Liu, Yi Song*, Baolei Tian, Junjie Qian, Yan Dong, Jilai Liu, Bin Liu and Zhixian Sun†

Department of Biochemistry and Molecular Biology, Beijing Institute of Radiation Medicine, 27 Taiping Road, Beijing 100850, China

*Yi Song, Department of Biochemistry and Molecular Biology, Beijing Institute of Radiation Medicine, 27 Taiping Road, Beijing 100850, China. Tel: +86 10 68214653, Fax: +86 10 68177417, email: songyibj@sina.com.cn

†Zhixian Sun, Department of Biochemistry and Molecular Biology, Beijing Institute of Radiation Medicine, 27 Taiping Road, Beijing 100850, China. Tel: +86 10 88628486, Fax: +86 10 68176833, email: sunzx@nic.bmi.ac.cn

It is well established that promyelocytic leukaemia nuclear bodies (PML NBs) play important roles in DNA damage responses (DDR). After irradiation, PML NBs dynamically recruit or release important proteins involved in cell-cycle regulation, DNA repair and apoptosis. As PML protein is the key molecule of PML NBs' dynamic assembling, we aimed to characterize the PML-interacting proteins in ^{60}Co-irradiated MCF-7 cells. A proteomic approach using CoIP, mono-dimensional electrophoresis and tandem mass spectrometry, allowed us to identify a total of 124 proteins that may associate with PML after irradiation. Bioinformatic analysis of the identified proteins showed that most of them were related to characterized PML functions, such as transcriptional regulation, cell-cycle regulation, cell-death regulation and response to stress. Four proteins, B23, MVP, G3BP1 and DHX9, were verified to co-localize with PML differentially before and after ionizing radiation (IR) treatment. The proteins identified in this study will significantly improve our understanding of the dynamic organization and multiple functions of PML NBs in DDR.

Keywords: DNA damage response/IR/PML NBs/ proteomic analysis.

Abbreviations: B23/NPM1, nucleophosmin; DDR, DNA damage response; DHX9/RHA, DEAH box protein 9/RNA helicase A; G3BP1, Ras-GTPase-activating protein SH3-domain-binding protein 1; IR, ionizing radiation; LC, liquid chromatography; MEF, mouse embryonic fibroblast; MVP/LRP, major vault protein/lung resistance-related protein; MS, mass spectrometry; PML, promyelocytic leukaemia protein; PML NBs, promyelocytic leukaemia nuclear bodies; SND1, Staphylococcal nuclease domain-containing protein 1.

There is nothing more fundamental than the genome for the existence and maintenance of living beings. To maintain the integrity of the genome, cells have evolved the ability to detect and propagate an initial DNA damage signal to elicit cellular responses that include cell-cycle arrest, DNA repair and apoptosis, which collectively have been termed the DNA damage response (DDR) (*1*). Dysregulation of the DDR machinery may lead to genetic diseases such as cancer. Ionizing radiation (IR), known as a DNA damaging agent, is also one of the mainstays of cancer therapy because it can trigger apoptosis (*2*). Defects in IR-induced cell death, therefore, not only increase the risk of cancer but also reduce the efficiency of cancer therapy. Thus, understanding the molecular mechanisms of IR-induced DNA damage response is critical for early cancer detection and potential treatments for cancer patients. Recent evidence suggests that promyelocytic leukaemia nuclear bodies (PML NBs) may be one of the key regulators in IR-induced DNA damage response: $PML^{-/-}$ mice are more sensitive to cancer-promoting drugs, cells derived from $PML^{-/-}$ mice showed strong resistance to γ-irradiation and apoptosis induced by IR was completely inhibited in $PML^{-/-}$ mouse embryonic fibroblast (MEF) cells (*3*).

PML NBs, also known as PML oncogenic domains (PODs), Kremer bodies or ND10s (nuclear dot 10s), are matrix-associated subnuclear multi-protein complexes. The promyelocytic leukaemia protein (PML) is the scaffold component of PML NBs and recruits onto these domains a striking variety of proteins, many of which are involved in apoptosis control (*3*). The most prominent feature of PML NBs is that they are highly dynamic and selectively recruit molecules under different conditions; it has been reported that close to 80 proteins can 'dock' to PML NBs in different contexts (http://npd.hgu.mrc.ac.uk/compartments/pml.html). Following DNA damage, PML NBs exchange their components with the surrounding nucleoplasm and other nuclear domains, allowing the cells to maintain the proper level and localization of various nuclear factors. Moreover, rather than merely serving as a docking site for transiting proteins, these bodies also serve as sites for post-translational modification of nuclear proteins (*4*). The dynamic changes of PML NB structure and protein content strongly imply a role for PML NBs in DDR. Due to the variety of proteins that PML regulates to translocate to or from the bodies, PML NBs have been implicated in transcriptional regulation, tumour suppression, senescence, DNA repair and apoptosis (*5*).

PML functionality, although enigmatic, remains intrinsically linked to its interacting proteins. Therefore, to understand the function of PML in the DDR, it is essential to characterize its dynamic interactions during specific stresses. As such, in this current study, using a combination of immunoprecipitation and mass spectrometry (MS), we analysed the composition of PML NBs in irradiation-treated MCF-7 cells. We identified a total of 124 proteins, which may localize to PML NBs after irradiation. Preliminary functional analysis confirms the plurifunctional nature of PML NBs.

Experimental Procedures

Cell culture and IR treatment

Cells were grown in Dulbecco's modified Eagle's medium (Invitrogen) supplemented with 10% foetal bovine serum (Hyclone, UT, USA), 2.4 g/l HEPES (Amresco) and 3.7 g/l sodium bicarbonate (Merck) in a 5% CO_2 humidified incubator at 37°C. For cell immunofluorescence studies, cells were subcultured on glass cover slips 1 day before use. IR treatments (at 10 Gy) were performed with ^{60}Co. Before ionizing irradiation, the culture medium was removed and the original medium was added to the cells. Cells were harvested at the indicated time points. For mock-treated control cells, the same procedure was followed without irradiation.

Western blot

For western blot analysis, cells were lysed in ice-cold RIPA buffer containing a complete protease inhibitor cocktail (Roche). After 1 h of gentle stirring at 4°C, samples were centrifuged at 12,000*g*, 4°C, for 20 min to remove insoluble material. After normalizing for protein concentration (BCA™ Protein Assay Kit; PIERCE), 40 μg of lysate was separated by 10% SDS–polyacrylamide gels, transferred to Hybond-ECL (GE Healthcare) and visualized by incubation with various primary antibodies and peroxidase-conjugated secondary antibodies (Invitrogen). The following antibodies were used for western blot analysis: mouse monoclonal anti-PML antibody (PG-M3; Santa Cruz), mouse monoclonal anti-B23 antibody (FC-8791; Santa Cruz), mouse anti-human G3BP1 (cat: 611126, lot: 39834; BD Transduction), mouse monoclonal anti-LRP/MVP antibody (1014, sc-23916; Santa Cruz), mouse monoclonal anti-DHX9 antibody (HOOOO1660-MO1; Abnova) and goat polyclonal anti-SND1/TudorSN antibody (C-17; Santa Cruz).

Immunofluorescence

Cells were grown on glass cover slips and treated as indicated. Cells were fixed in 4% paraformaldehyde/PBS (pH 7.5) for 15 min before permeabilization in 0.5% Triton X-100 in PBS for 5 min at room temperature. After blocking in goat serum, the cells were incubated with the indicated antibody, followed by incubation with Alexa Fluor 488 goat anti-mouse or Alexa Fluor 555 goat anti-rabbit IgG (H + L) (Molecular Probes, Invitrogen) and DAPI. The antibodies used for immunofluorescence microscopy were: mouse monoclonal anti-PML antibody (PG-M3; Santa Cruz), anti-rabbit PML (H238; Santa Cruz), mouse monoclonal anti-B23 antibody (FC-8791; Santa Cruz), mouse anti-human G3BP1 (cat: 611126, lot: 39834; BD Transduction) and mouse monoclonal anti-LRP/MVP antibody (1014, sc-23916; Santa Cruz). Images were acquired using immunofluorescence microscopy (OLYMPUS).

Immunoprecipitation

Both mock- and IR-treated cells were lysed in M-PER® Mammalian Protein Extraction Reagent (Roche), supplemented with a complete protease inhibitor cocktail. The lysate was first pre-cleared by incubation with protein A/G PLUS-Agarose beads (sc-2003; Santa Cruz) and anti-mouse/goat IgG for 4 h, then incubated with anti-mouse/goat IgG or anti-mouse/goat PML antibody (PG-M3; E15; Santa Cruz) for 2 h before incubation with protein A/G-Sepharose overnight at 4°C. Immunoprecipitates were washed four times with ice-cold NETN buffer (20 mM Tris–HCl pH 8.0, 1 mM EDTA, 0.5% NP-40, 150 mM NaCl, protease-inhibitor cocktail) and resolved by SDS-PAGE.

In-gel trypsin digestion

Immunoprecipitated proteins from both mock-treated and irradiated MCF-7 cells were separated by 10% SDS–polyacrylamide gels and stained with Coomassie Brilliant Blue G-250 dye (cat: 17524; Serva) After image analysis, the protein bands of interest were cut out of the gel and minced into pieces. The gel pieces were de-stained with 50% ACN in 25 mM ammonium bicarbonate until transparent and then dried in a vacuum centrifuge. Protein spots were incubated with 60–80 μl trypsin (0.01 μg/μl, 25 mM ammonium bicarbonate) for 16–18 h at 37°C. The gel straps were immersed in 50 μl of 0.5% TFA, 50% ACN for 1 h at 37°C, followed by another 50 μl of 0.5% TFA, 50% ACN for 1 h at 37°C. The supernatant was combined and vacuum dried.

LC MS/MS analysis and database searching

The chromatography experiments were performed on a NanoACQUITY UPLC ultra-HPLC system (Waters) equipped with an autosampler. The affinity column was Symmetry C18 (180 μm × 20 mm, particle size: 5 μm) and the analytical column was NanoACQUITY UPLC BEH C18 (75 μm × 250 mm, particle size: 1.7 μm). Solvent A was composed of 0.1% FA, 99.9% H_2O and solvent B was composed of 0.1% FA, 99.9% ACN. The gradient was performed as follows: 0–50 min, 1–40% B; 50–60 min, 40–60% B; 60–70 min, 60% B; 70–90 min, 1% B. MS^n experiments were performed on Synapt high definition mass spectrometry (HDMS) (Waters) equipped with a nanospray source. The mass spectrometer was operated in DDA mode and the two most abundant ions detected in the scan were analysed by MS2 scan events. The data were processed by PLGS v2.3 and searched against the IPI database (Human_3.51) by Mascot.

The search parameters were as follows: trypsin digestion with one missed tryptic cleavage site; carbamidomethyl as a variable modification for cysteines and oxidation as a variable modification for methionines; the MS tolerance and MS/MS tolerance were both 50 ppm. The criteria for protein identification were as follows: the protein score was significant ($P < 0.05$) and >60 and at least two different peptide sequences matched.

RNA interference

The target sequence of B23 siRNA was selected as follows 5′-AGAU GAUGACGAUGAUGAUTT-3′. As a negative control, a Nc siRNA duplex with the sequence 5′-UUCUCCGAACGUGUCAC GUdTdT-3′ was used. Both of them were synthesized by Shanghai GenePharma Co., Ltd. Proliferating MCF-7 cells were transfected with the 100 nM B23 siRNA or 100 nM Nc siRNA by using the INTERFERin siRNA transfection reagent (Polyplus) according to the manufacturer's protocol. After 48 h, the cells were ready for gene knockdown analysis and immunofluorescence staining.

Results

Location and number of PML NBs were dynamically regulated by irradiation

To improve the detection rate of low-abundance PML protein and the success rate of MS identification, we first surveyed the expression of PML in 13 cell lines (Supplementary Fig. 1S) and chose MCF-7 cells with higher PML expression for further study. To obtain results that could reveal the dynamic components in PML NBs in irradiation responses, we monitored the number and subcellular distribution of PML NBs before and after irradiation by immunofluorescence. MCF-7 cells were fixed before or at 0.5, 3, 6, 12 or 24 h after irradiation (10 Gy) and the number of PML NBs in 100 cells was calculated at each time point. We found that the number of PML NBs was significantly up-regulated by irradiation in MCF-7 cells in a time-dependent manner, peaking at 6 h after

irradiation (Fig. 1A and B). Thus, un-irradiated cells and cells irradiated for 6 h were collected for co-immunoprecipitation and MS.

IR-induced changes in PML-interacting protein profile

The efficiency of this specific enrichment was also confirmed by western blot analysis of the different protein immunoprecipitates with the specific anti-PML mouse monoclonal antibody (PG-M3; Santa Cruz). Protein samples from unfractionated whole-cell extract, immunoprecipitate from MCF-7 cells by mouse monoclonal IgG immunoglobulin and immunoprecipitates from both mock-treated and irradiated MCF-7 cells by mouse monoclonal anti-PML antibody (PG-M3; Santa Cruz) were separated by SDS–PAGE, transferred to a nitrocellulose membrane and probed with the same antibody used for PML precipitation. As shown in Fig. 2, PML was detected in total cell extract and was highly enriched in the anti-PML immunoprecipitation fraction and there was a little more abundant accumulation of PML in the immunoprecipitated fraction of irradiated cells, consistent with the aforementioned increase in number of PML NBs

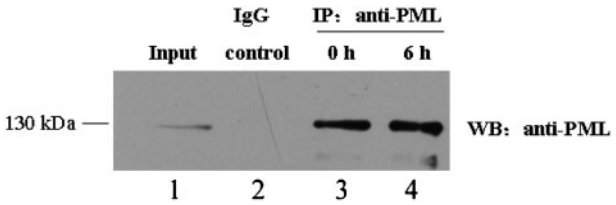

Fig. 2 Effectiveness of specific enrichment for PML by immunoprecipitation. Western blot analysis of the whole-cell extract and the different immunoprecipitates treated with the preclearing process. Lane 1: the whole-cell extract as input control; Lane 2: immunoprecipitate generated using mouse IgG from mock-treated MCF-7 cells; Lanes 3 and 4: immunoprecipitates generated using the mouse monoclonal anti-PML antibody (PG-M3; Santa Cruz) from mock- (*3*) and IR-treated (*4*) MCF-7 cells, respectively.

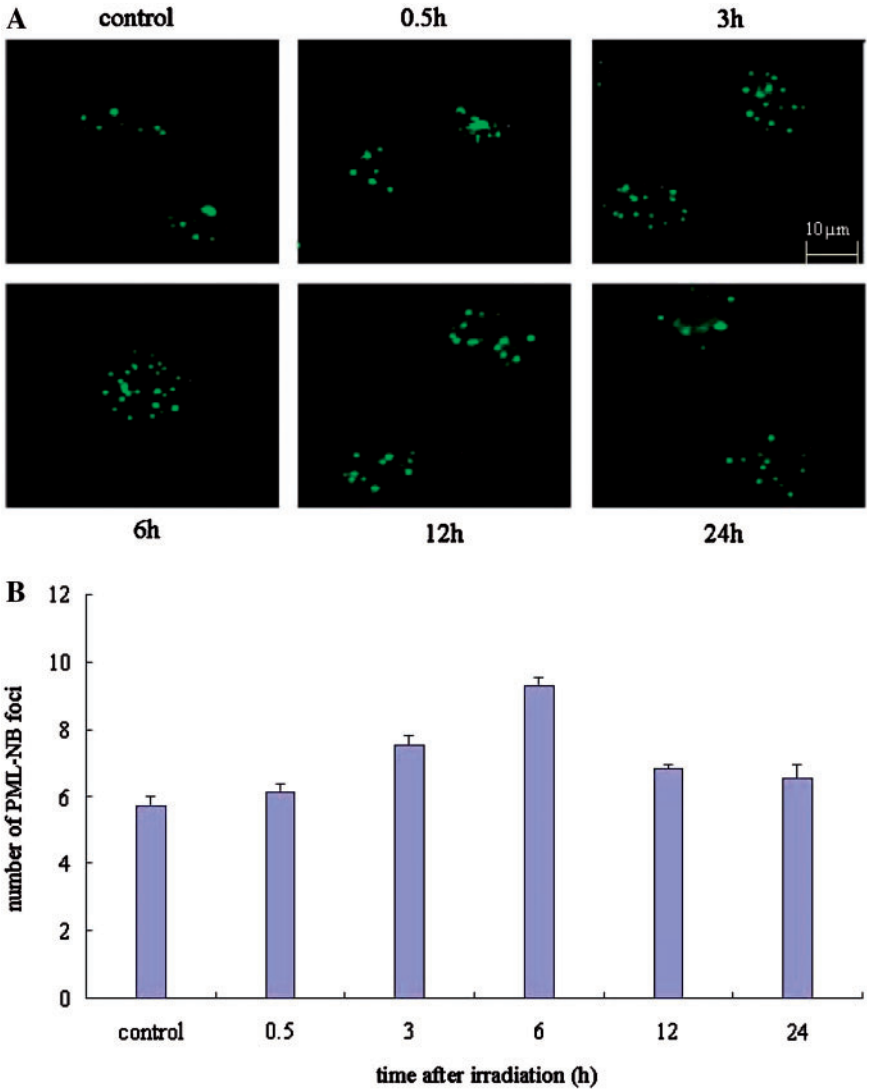

Fig. 1 Dynamics of PML expression before or after γ-irradiation. (A) Dynamics of PML NBs following γ-irradiation. After IR treatment, PML NBs rapidly increase in number. MCF-7 cells were fixed before and at 0.5, 3, 6, 12 and 24 h after irradiation. Antibodies against PML (PG-M3; Santa Cruz) were used for immunofluorescence (green). (B) Analysis of the number of PML NBs before and after irradiation in MCF-7 cells. Values are means of triplicates (±SD). The figure is representative of the results obtained in 3 independent experiments.

after irradiation. As expected, PML was not detected in the control lane containing immunoprecipitate produced from untreated MCF-7 cells by mouse IgG, illustrating that the immunoprecipitation process we optimized was specific and successful.

Proteomic analysis of the PML-interacting proteins

Proteins from PML NBs isolated by immunoprecipitation from both mock-treated and irradiated MCF-7 cells were separated by one-dimensional SDS–PAGE and stained with Coomassie Blue G-250 dye. The band patterns obtained from the immunoprecipitates were similar for both mock-treated and irradiated nuclear bodies, as seen by SDS–PAGE (Fig. 5A, lanes 1 and 2). However, there were some protein bands whose intensity in the irradiated nuclear bodies was markedly increased relative to the control nuclear bodies. These bands were sequentially excised, in-gel digested with trypsin and analysed by liquid chromatography (LC) MS/MS. A total of 124 proteins were identified using the criteria described in 'Experimental Procedures' section. The name of the proteins identified and their database accession numbers are reported in Supplementary Table 1S. Of the 124 identified proteins, 7 proteins (Table I) were annotated as PML-NB components in the nuclear protein database (http://npd.hgu.mrc.ac.uk/compartments/pml.html) and 8 proteins were homologous to known PML-NB localized proteins (Table II). The efficiency of this specific enrichment was also confirmed by the identification of PML protein itself by MS (Table I). This further demonstrated that the immunoprecipitation was effective and specifically enriched for the PML NBs, meaning that the MS data obtained could be used for advanced analysis.

Functional classification of the identified proteins

To evaluate the reliability of the data we had gotten, we carried out extensive bibliographic and bioinformatic analyses for the 124 proteins. Functional annotations of these newly identified putative PML-interacting proteins were assigned according to gene ontology (http://www.hupo.org.cn/GOfact). Each of the identified proteins was categorized by criteria such as molecular function and cellular process (Fig. 3). Out of the 124 identified proteins, 94 (75.8%) have cellular process annotations (Fig. 3A) and 105 (84.6%) exhibit at least one known biological function (Fig. 3B); most of the 124 proteins are involved in the regulation of crucial physiological processes. Altogether, the cellular processes in which these 105 annotated proteins are involved are consistent with the roles that PML NBs play in biological processes (*5*), including cellular signal transduction, metabolism, proliferation, differentiation and development. Proteins associated with metabolism fall into the major functional category that corresponds to PML NB function, namely, protein degradation. The largest category of protein function annotations is protein-binding functionality, consistent with the known role of PML NBs in serving as depots or storage sites for nuclear proteins, allowing the sequestered proteins to interact with one another. The different classes resulting from these analyses and the percentage of proteins contained in each class are presented in Fig. 3B. Collectively, these results suggest that the identified proteins are closely implicated in the biological activities of PML NBs.

Although MS could identify the components of PML NBs, the topology of the protein organization was difficult to determine. To obtain the crucial foundation for modelling and data reduction, we used the STRING database to analyse the functional relationships between the identified proteins and PML. Of the 124 identified proteins, 51 proteins, which are involved in cellular processes such as stress reaction, nucleic acid metabolism, protein degradation, cell-cycle regulation and apoptosis, were selected for STRING database searching (http://string.embl.de/). Among the 24 proteins that the STRING database could recognize, only 15 proteins have a functional association, most likely mediating cellular stress reactions, as shown in Fig. 4. As expected, database retrieval merely displayed the PML interaction network to some degree. Limited by the speed of database updating, some reported interactions, such as the interactions between PML and DHX9 (*6*), were not assigned in the STRING database. Thus, a more refined network depiction requires more literature-mining searches and experimental testing.

Verification of characterized proteins

Based on the above bioinformatic analyses and assessment of the PML interaction data, we further verified the MS results with experimental testing. Five newly identified proteins (Fig. 4), which have high likelihood of interacting with PML based on high MS score, nuclear localization and participation in cell proliferation, cell-cycle regulation or stress response (Supplementary Table 2S), were selected for advanced confirmation. IP-WB analysis showed that four of the five proteins were co-immunoprecipitated with PML, suggesting that these four proteins are

Table I. Known PML-NB localized proteins identified in this study.

Protein name	Protein accession number	Protein score
PML	IPI00022348	561
RPA1 70K	IPI00020127	280
RPA2 32K	IPI00013939	69
DHX9	IPI00844578	520
PARP-1	IPI00449049	65
AP-1	IPI00328257	85
HP1 beta	IPI00021924	60

Table II. Novel PML-interacting proteins identified in this study that are homologues of known PML-NB components.

Identified proteins	Known PML-NB localized proteins
ZFP147	ZFP198, ZFP506
EIF2S1, eIF-4D, EIF2AK1	EIF4E
DHX30, DHX16	DHX9
M4	M1

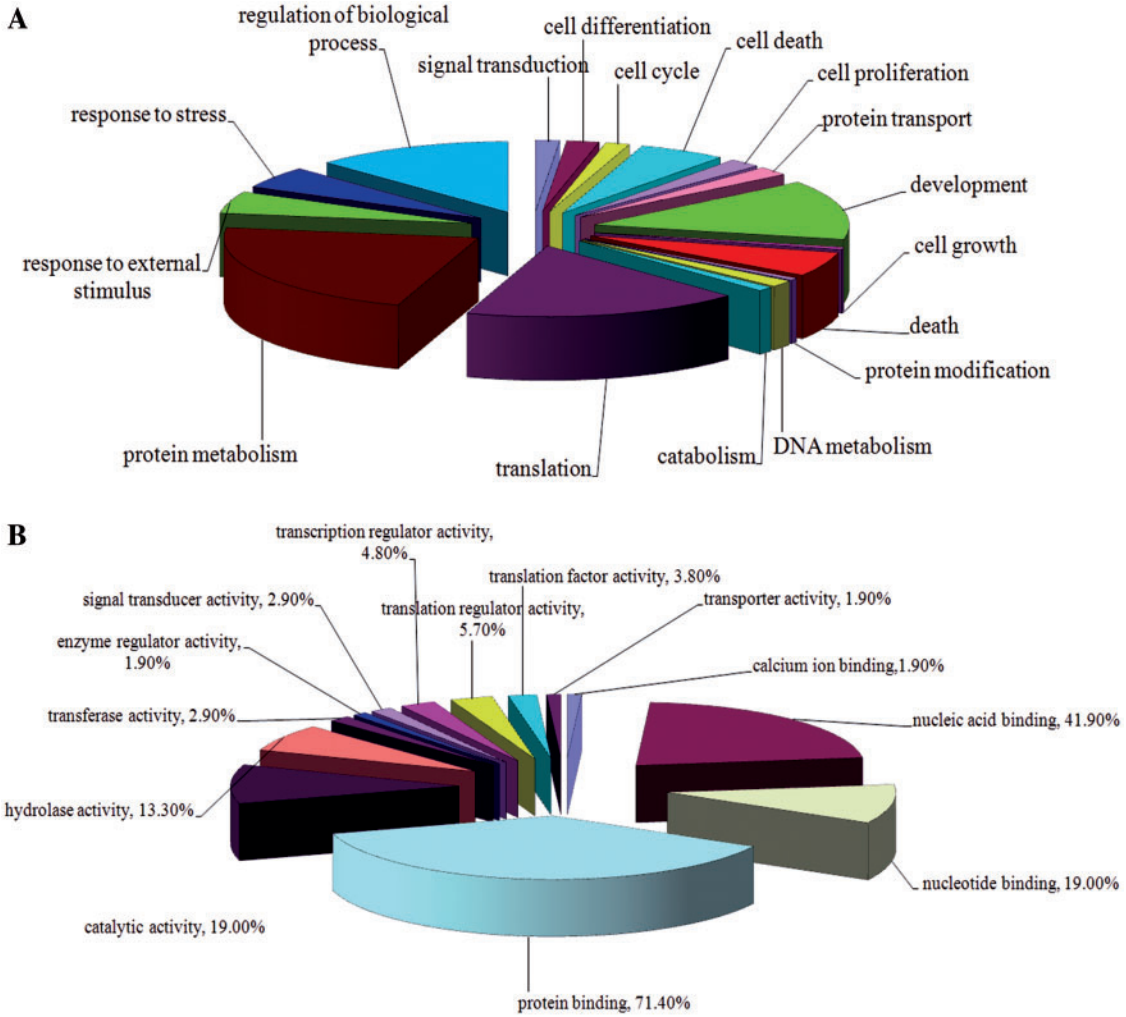

Fig. 3 Functional classification putative PML-interacting proteins identified in this study. (A) The 124 identified proteins categorized by cellular process. (B) Outline of the molecular functional categories of the 124 proteins identified in this study. The name of the class is given, followed by the percentage of the 124 proteins that fall into each class.

PML-interacting proteins. Moreover, these proteins differentially interacted with PML pre- and post-irradiation.

As shown in Fig. 5, B23 and G3BP1 are present in PML-immunoprecipitates from irradiation-treated cells (Fig. 5A, lane b) but are not detectable in immunoprecipitates from control cells (Fig. 5A, lane a). On the other hand, MVP and DHX9 are present in both cases but exhibit reduced mobility upon irradiation induction. These differences could result from protein modifications that alter the running behaviour of proteins in SDS–PAGE. Since PML NBs can function as depots for protein modification and since both MVP and DHX9 can be modulated by multiple post-translational modifications, this hypothesis is not surprising. Consistent with this hypothesis, Fuchsová *et al.* (*6*) also found that DHX9 was recruited to PML NBs following IFN treatment. Of the proteins selected for validation, only the protein SND1 was not detected in the PML complex, indicating that our data were highly reliable.

Additionally, to address whether these classes of proteins are genuine components of PML NBs *in vivo*, we further examined the subcellular distribution of the verified proteins B23, G3BP1 and MVP in irradiated MCF-7 cells using fluorescence microscopy. Immunofluorescence localization of these three proteins revealed that consistent with the CoIP-WB results (Fig. 5A, lane a), B23 and G3BP1 did not co-localize with PML, MVP co-localized with PML before irradiation. After irradiation, the nuclear G3BP1 and MVP both concentrated in PML NB speckles; while B23 partially co-localized with PML foci (Fig. 5B). To further confirm the functional interaction between PML and B23, we down-regulate B23 expression by using specific B23 siRNA in MCF-7 cells, which results in the obvious increase of the number of PML immunofluorescence foci (PML NBs) compare with Nc siRNA transfected control cells, indicating the involvement of B23 in regulating the number of PML NBs (Fig. 6).

Taken together, we concluded that these four proteins, B23, G3BP1, MVP and DHX9, are novel components of the PML NBs; furthermore, their novel associations with PML NBs are involved in the IR-induced DNA damage response.

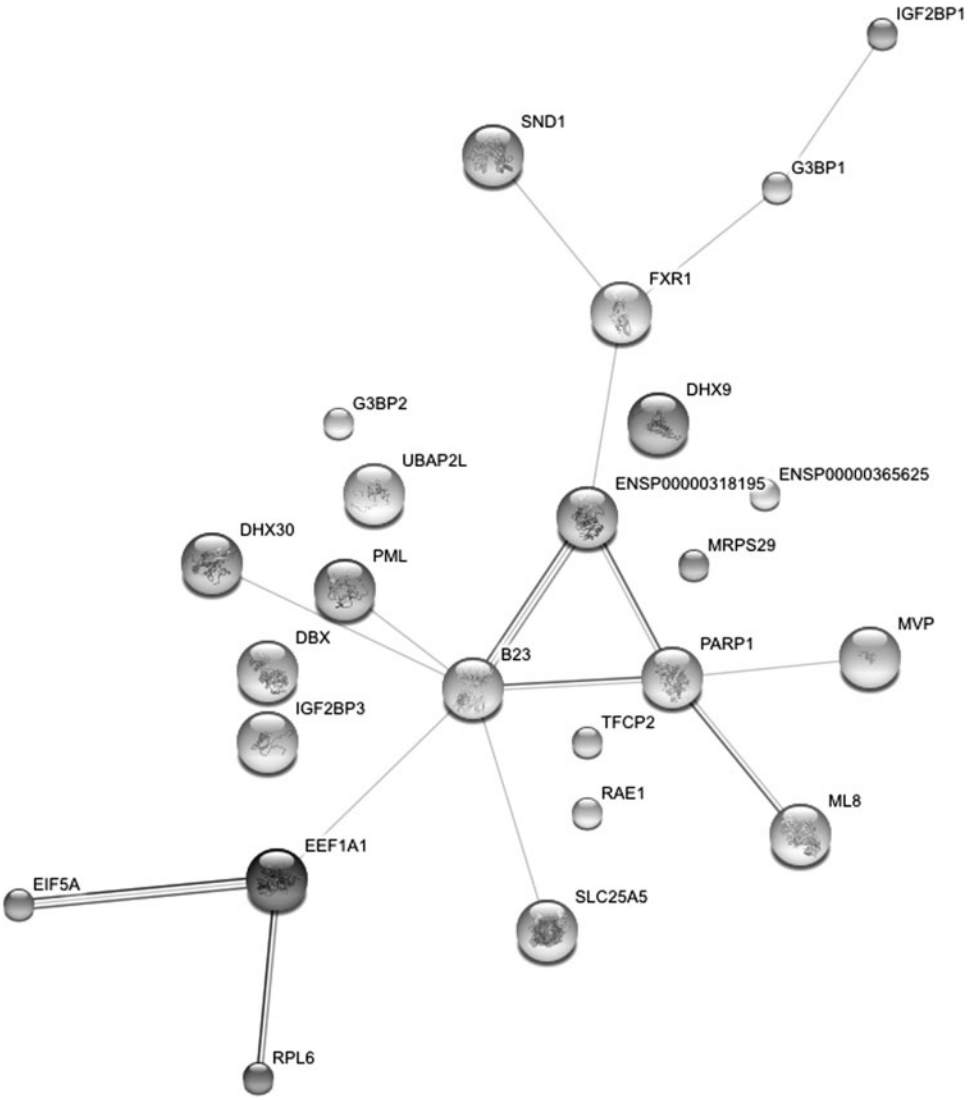

Fig. 4 Analysis of high-confidence PML-interacting proteins by STRING database. Of the 24 proteins recognized by the database, 15 were functionally connected, providing intuitive visual scaffolds for annotating the PML signalling pathway. In this network, SND1, G3BP1, DHX9, MVP and B23 were selected for further verification.

Discussion

Since Bernstein (*7*) described PML NBs as atypical speckles for the first time in 1984, many approaches have been employed to elucidate the multiple functions of PML NBs. However, the molecular mechanisms governing the assembly and activity of PML NBs in DNA damage responses are still ill-defined. Unquestionably, identification of proteins contained within PML NBs represents one of the first indispensable steps toward completing this tremendous task. Here, we report a large-scale characterization of PML-NB components in IR-treated MCF-7 cells. Our study represents the first and largest functional proteomic analysis reported so far for PML NBs. A total of 124 proteins were identified to locate in the PML NBs after irradiation. Almost certainly in any CoIP experiment there are non-specific background proteins being isolated, therefore, at this stage of the study, we cannot exclude that some of these proteins are found artifactually within the PML NBs; however, the results of this study are useful, as it provides detailed catalogues of the PML-NB components to seek for the potential candidate proteins responsible for DNA damage response regulation.

The first step of our proteomic analysis of PML NBs was to enrich for PML-interacting proteins from MCF-7 cells and to improve their purity as much as possible. At present, different approaches have been used to characterize protein complexes and protein–protein interaction networks. Blue native polyacrylamide gel electrophoresis (BN-PAGE) (*8*, *9*) separates native proteins and protein complexes by conferring a negative charge on all proteins via the dye Coomassie blue. The separation depends mainly on the size of the protein complex and this method can be used for protein complexes from 10 kDa to 10 MDa. The limitations of this method are restrictions of the size of separated protein complexes and lower resolution of protein complexes with similar

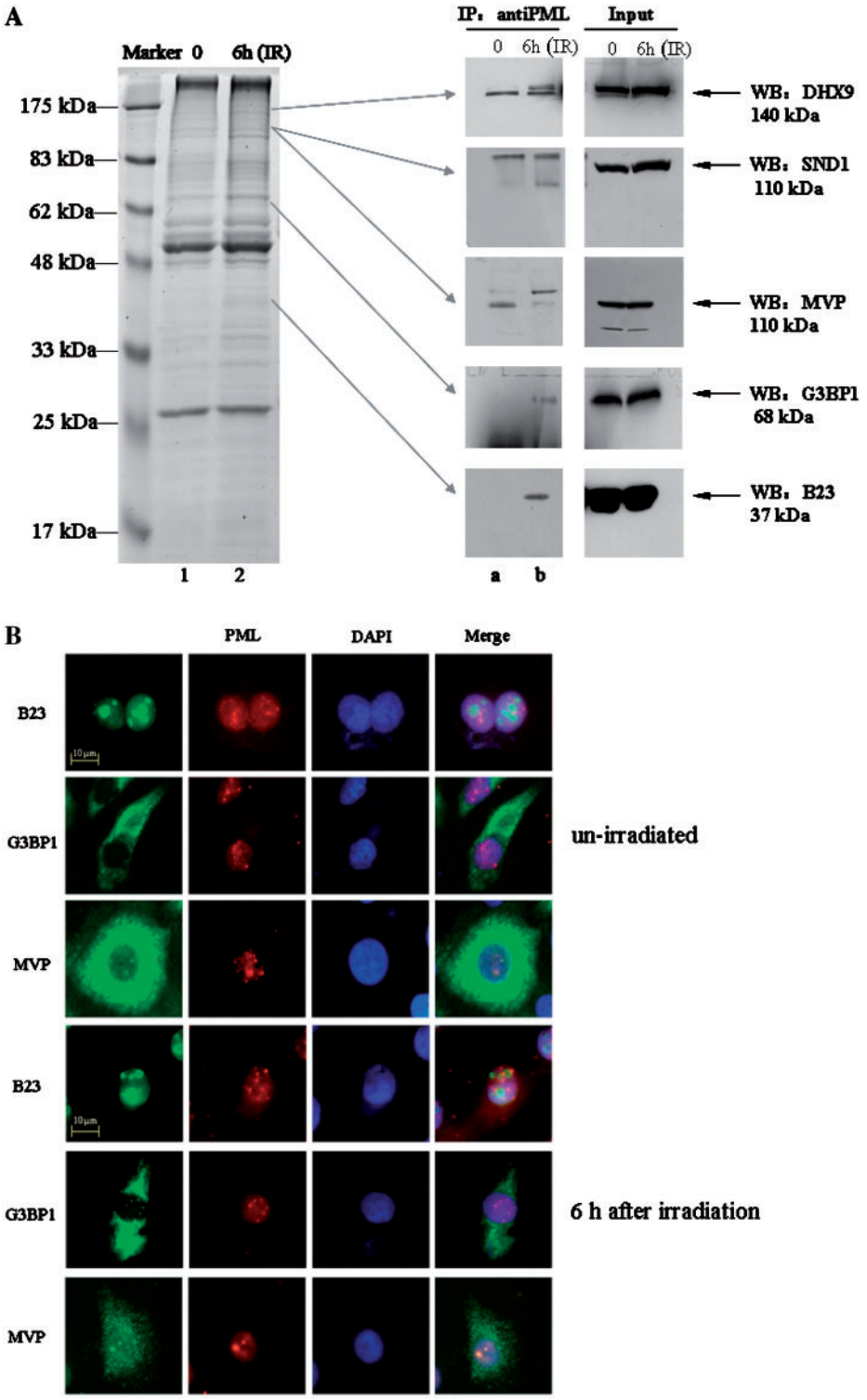

Fig. 5 Association between PML and newly identified putative PML-interacting proteins. (A) Endogenous DHX9, MVP, G3BP1 and B23 were co-immunoprecipitated with PML. Cell lysates were immunoprecipitated (IP) using mouse anti-PML antibody (PG-M3; Santa Cruz), followed by immunoblot (IB) using antibodies against RHA, SND1, MVP, G3BP1 and B23. (B) MVP, G3BP1 and B23 partially co-localized with PML. MCF-7 cells were collected before and at 6 h after irradiation. Immunofluorescence staining was performed using antibodies against MVP, G3BP1 or B23 (green), PML (H238; Santa Cruz) (red) and the DAPI nuclear staining (blue).

molecular masses. Since PML NBs have been shown to contain close to 80 proteins and since it is estimated that microstructures formed as a result of fission or budding from the surface of parental PML NBs have a molecular mass of 0.5–5 MDa (*10*), BN-PAGE may not sufficiently separate such macromolecular complexes. A two-hybrid system may produce false positive interactions when protein domains are inappropriately exposed due to altered folding. In addition, not all proteins are amenable to two-hybrid

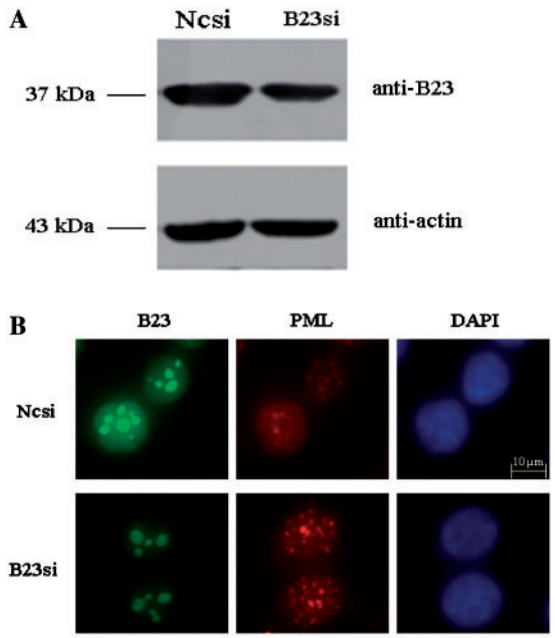

Fig. 6 PML NBs number was increased in B23 knockdown cells. (A) The expression of B23 was inhibited by siRNAs. MCF-7 cells were respectively transfected with 100 nM negative control siRNA or 100 nM B23 siRNA for 48 h. The expression of B23 was detected by western blot with anti-B23 antibody (up), using actin as the internal control (down). (B) B23 functions in regulating the number of PML NBs. Immunofluorescence staining of B23 and PML were performed in B23 knockdown cells and negative control cells. Increasing number of PML-NB foci was observed in B23 knockdown cells.

analysis. More recently, the TAP approach (*11*) has been developed to isolate multi-protein complexes. Proteins of interest are expressed with an epitope tag, which is then used as an affinity handle to purify the tagged protein along with its interacting partners. However, the epitope added to the target protein may affect protein conformation and perturb the physiological protein–protein interactions. To circumvent all of these problems, we chose the co-immunoprecipitation method to isolate endogenous PML NBs under native conditions. PML exists as a collection of markedly different protein isoforms and the anti-PML antibody used for co-immunoprecipitation recognizes the N-terminal sequence of PML, which is shared by all its splice variants, theoretically allowing us to detect all isoforms of PML. However, the anti-PML antibody we used here mainly detected a single protein band in western blot (Fig. 2) and showed the typical speckled distribution of PML NBs when used for immunofluorescence detection of PML in the cell (Fig. 1A), suggesting that this antibody has more specific recognition of a structural PML isoform involved in PML NB formation and that most of the PML-interacting proteins identified through immunoprecipitation are the ones localized to PML NBs. Immunofluorescence of B23, MVP and G3BP1 showed colocalization with PML NBs (Fig. 5B); this provides further evidence that we successfully obtained the multi-protein complexes of PML NBs.

One of the crucial roles of PML is to modulate the activity of p53, which is the core transcription factor in the DNA damage response and determines whether the cells live or die. Remarkably, PML and PML NBs appear to regulate p53 transcriptional activity in response to genomic damage by providing a platform for post-translational modification of the p53 protein, thus activating transcription of apoptosis-promoting genes or suppressing transcription of apoptosis-resisting genes to induce cell death (*12*). Recent work has demonstrated colocalization of PML and p53 at the sites of DNA breaks (*13*), implicating the PML NBs in the recognition and/or processing of DNA breaks via recruitment of p53, which is required for both checkpoint and DNA repair responses. Hence, the PML-p53 network is thought to be one of the key mechanisms of guarding genomic stability. Interestingly, the three novel PML-interacting proteins identified here, G3BP1 (*14*), B23 (*15*) and MVP (*16*), can also regulate the function of p53 either directly or indirectly. Since the three proteins we verified have connections with both PML and p53, the next question is whether these proteins are involved in the PML-p53 regulation network. It will therefore be important to reveal whether and how these proteins participate in the PML-p53 regulation network. In addition, the association between B23 and PML was identified after irradiation. In addition to radiation, the interaction between PML and B23 may also be induced by other stress agents. Knocking-down B23 expression by siRNA may also be considered as a kind of stress of the cells. It has been reported that down-regulation of B23 in HL-60 cells attributed to apoptosis induced by BuONa/vanadate. As PML plays important roles in p53-dependent and independent apoptosis signalling in mammalian cells, the impairment of PML in B23si cells is reasonable in this process and in accordance with the fact that tumour tissue samples always have high B23 and low PML expression. Naturally, more studies are needed to reveal the precise functional relationships underlying B23-PML interaction. A detailed analysis of the *in vivo* function of these interactions is beyond the scope of this study but will be addressed in our future work.

Intriguingly, PML has also been implicated in p53-independent apoptosis (*17*), a connection that adds further layers of complexity to our knowledge of PML. So far, little is known about the molecular mechanism by which PML regulates these processes. In this respect, proteins identified in 'remote relationship' with p53 are equally noteworthy and many more experiments will be required to address this question.

In conclusion, although more work remains to be done, the proteome of PML NBs presented here will help to draw a more detailed picture about the role of PML NBs in DNA damage response regulation and tumour suppression. This may allow us to develop potential therapeutic strategies to prevent and treat cancer in the near future.

Supplementary Data

Supplementary Data are available at *JB* Online.

Funding
The Chinese National Key Program for Developing Basic Research (2007CB914604);The Chinese National Natural Sciences Foundation Projects (30600162, 30600109 and 30900276).

Conflict of interest
None declared.

References

1. Bartek, J., Bartkova, J., and Lukas, J. (2007) DNA damage signalling guards against activated oncogenes and tumour progression. *Oncogene* **26**, 7773–7779
2. Karagiannis, T.C. and El-Osta, A. (2004) Double-strand breaks: signaling pathways and repair mechanisms. *Cell Mol. Life Sci.* **61**, 2137–2147
3. Takahashi, Y., Lallemand-Breitenbach, V., Zhu, J., and de Thé, H. (2004) PML nuclear bodies and apoptosis. *Oncogene* **23**, 2819–2824
4. Dellaire, G. and Bazett-Jones, D.P. (2004) PML nuclear bodies: dynamic sensors of DNA damage and cellular stress. *BioEssays* **26**, 963–977
5. Salomoni, P., Ferguson, B.J., Wyllie, A.H., and Rich, T. (2008) New insights into the role of PML in tumour suppression. *Cell Res.* **18**, 622–640
6. Fuchsová, B., Novák, P., Kafková, J., and Hozák, P. (2002) Nuclear DNA helicase II is recruited to IFN-α-activated transcription sites at PML nuclear bodies. *J. Cell Biol* **158**, 463–473
7. Bernstein, R.M. (1984) Antinuclear antibodies in primary biliary cirrhosis. *Lancet* **1**, 508
8. Wittig, I., Braun, H.P., and Schägger, H. (2006) Blue native PAGE. *Nat. Protoc.* **1**, 418–428
9. Krause, F. (2006) Detection and analysis of protein–protein interactions in organellar and prokaryotic proteomes by native gel electrophoresis: (Membrane) protein complexes and supercomplexes. *Electrophoresis* **27**, 2759–2781
10. Eskiw, C.H., Dellaire, G., Mymryk, J.S., and Bazett-Jones, D.P. (2003) Size, position and dynamic behavior of PML nuclear bodies following cell stress as a paradigm for supramolecular trafficking and assembly. *J. Cell Sci.* **116**, 4455–4466
11. Krogan, N.J., Cagney, G., Yu, H., Zhong, G., Guo, X., Ignatchenko, A., Li, J., Pu, S., Datta, N., Tikuisis, A.P., Punna, T., Peregrín-Alvarez, J.M., Shales, M., Zhang, X., Davey, M., Robinson, M.D., Paccanaro, A., Bray, J.E., Sheung, A., Beattie, B., Richards, D.P., Canadien, V., Lalev, A., Mena, F., Wong, P., Starostine, A., Canete, M.M., Vlasblom, J., Wu, S., Orsi, C., Collins, S.R., Chandran, S., Haw, R., Rilstone, J.J., Gandi, K., Thompson, N.J., Musso, G. St, Onge, P., Ghanny, S., Lam, M.H., Butland, G., Altaf-Ul, A.M., Kanaya, S., Shilatifard, A., O'Shea, E., Weissman, J.S., Ingles, C.J., Hughes, T.R., Parkinson, J., Gerstein, M., Wodak, S.J., Emili, A., and Greenblatt, J.F. (2006) Global landscape of protein complexes in the yeast Saccharomyces cerevisiae. *Nature* **440**, 637–643
12. Gottifredi, V. and Prives, C. (2001) P53 and PML: new partners in tumor suppression. *Trends Cell Biol.* **11**, 184–187
13. Carbone, R., Pearson, M., Minucci, S., and Pelicci, P.G. (2002) PML NBs associate with the hMre11 complex and p53 at sites of irradiation induced DNA damage. *Oncogene* **21**, 1633–1640
14. Kim, M.M., Wiederschain, D., Kennedy, D., Hansen, E., and Yuan, Z.M. (2007) Modulation of p53 and MDM2 activity by novel interaction with Ras-GAP binding proteins (G3BP). *Oncogene* **26**, 4209–4215
15. Gjerset, R.A. (2006) DNA damage, p14ARF, Nucleophosmin (NPM/B23), and cancer. *J. Mol. Hist.* **37**, 239–251
16. Yi, C., Li, S., Chen, X., Wiemer, E.A., Wang, J., Wei, N., and Deng, X.W. (2005) Major vault protein, in concert with constitutively photomorphogenic 1, negatively regulates c-Jun-mediated activator protein 1 transcription in mammalian cells. *Cancer Res.* **65**, 5835–5840
17. Bernardi, R. and Pandolfi, P.P. (2003) Role of PML and PML-nuclear body in the control of programmed death. *Oncogene* **22**, 9048–9057